Biomaterials 33 (2012) 2223–2229

Contents lists available at SciVerse ScienceDirect

Biomaterials

journal homepage: www.elsevier.com/locate/biomaterials

Amphiphilic micelles of poly(2-methyl-2-carboxytrimethylene carbonate-*co*-D,L-lactide)-*graft*-poly(ethylene glycol) for anti-cancer drug delivery to solid tumours

Karyn S. Ho [a], Ahmed M. Aman [b], Rima S. Al-awar [b], Molly S. Shoichet [a,c,*]

[a] Terrence Donnelly Centre for Cellular and Biomolecular Research, Department of Chemical Engineering & Applied Chemistry, Institute of Biomaterials & Biomedical Engineering, University of Toronto, Room 514, 160 College Street, Toronto, ON M5S 3E1, Canada
[b] Medicinal Chemistry, Ontario Institute for Cancer Research, 101 College Street, Toronto, ON M5 G 1L7, Canada
[c] Department of Chemistry, University of Toronto, 80 St. George Street, Toronto, ON M5S 3H6, Canada

ARTICLE INFO

Article history:
Received 4 November 2011
Accepted 25 November 2011
Available online 17 December 2011

Keywords:
Polymeric nanoparticles
In vivo evaluation
Micelle
Self-assembly
Chemotherapy
Drug delivery

ABSTRACT

Drug delivery to solid tumours remains a challenge because both tumour physiology and drug solubility are unfavourable. Engineered materials can provide the basis for drug reformulation, incorporating active compounds and modulating their pharmacokinetic and biodistribution behaviour. To this end, we encapsulated docetaxel, a poorly soluble taxane drug, in a self-assembled polymeric nanoparticle micelle of poly(2-methyl-2-carboxytrimethylene carbonate-*co*-D,L-lactide)-*graft*-poly(ethylene glycol) (poly(TMCC-*co*-LA)-*g*-PEG). This formulation was compared with its conventional ethanolic polysorbate 80 formulation in terms of plasma circulation and biodistribution in an orthotopic mouse model of breast cancer. Notably, the polymeric nanoparticle formulation achieved greater tumour retention, resulting in prolonged exposure of cancer cells to the active drug. This behaviour was unique to the tumour tissue. The active drug was eliminated at equal or greater rates in all other tissues assayed when delivered in the polymeric nanoparticles vs. the free drug formulation. Thus, these polymeric nanoparticles are promising vehicles for solid tumour drug delivery applications, offering greater tumour exposure while eliminating the need for toxic solvents and surfactants in the dosing formulation.

1. Introduction

Solid tumours, such as breast cancer, present several physical barriers against effective drug delivery, as therapeutic agents must cross into, and remain, at the tumour site despite high interstitial pressures and low vascular densities [1–3]. Additionally, many anti-cancer drugs have non-specific modes of action, so when coupled with a broad systemic distribution, the resulting impact on healthy cells leads to dose-limiting toxicity [4]. Nanoparticle targeting exploits a unique physiological feature of solid tumours resulting from rapid malignant growth: hyperpermeable vasculature and poor lymphatic drainage lead to enhanced permeability and retention (EPR) of large molecules and small particles on the nanometer scale, providing a means for selective tissue accumulation [5,6]. Well-designed nanoscale drug delivery systems have the potential to increase the therapeutic index of small molecule drugs by extending drug circulation while boosting solid tumour specificity and accumulation through the EPR effect. To take advantage of EPR, several technologies have been developed, including liposomes [7], dendrimers [8], and polymeric nanoparticles [9].

Polymeric nanoparticles, comprised of a hydrophobic core and hydrophilic corona, are particularly compelling for the encapsulation and delivery of hydrophobic and poorly water soluble chemotherapeutic drugs. Many of these polymers are block copolymers of hydrophobic poly(aspartic acid) or poly(lactide-*co*-glycolide) and hydrophilic poly(ethylene glycol) [10,11]. Several parameters have been investigated in terms of circulation half-life, including the length and density of the PEG block [12] and size and shape of the nanoparticles [13,14]. Interestingly few polymeric nanoparticles have been designed with functional groups.

The copolymer poly(2-methyl-2-carboxytrimethylene carbonate-*co*-D,L-lactide)-*graft*-poly(ethylene glycol) (poly(TMCC-*co*-LA)-*g*-PEG) was designed to have either a PEG-furan or a PEG-azide for facile click modification of the nanoparticle surface by either Diels-Alder [15] or Huisgen 1,3-dipolar cycloaddition [16], respectively. By combining the hydrophobic backbone of poly(TMCC-*co*-LA) with

* Corresponding author. Terrence Donnelly Centre for Cellular and Biomolecular Research, Department of Chemical Engineering & Applied Chemistry, Institute of Biomaterials & Biomedical Engineering, University of Toronto, Room 514, 160 College Street, Toronto, ON M5S 3E1, Canada. Fax: +1 416 978 8287.
E-mail address: molly.shoichet@utoronto.ca (M.S. Shoichet).

0142-9612/$ – see front matter © 2011 Elsevier Ltd. All rights reserved.
doi:10.1016/j.biomaterials.2011.11.072

hydrophilic PEG, the resulting amphiphilic copolymer spontaneously self-assembles into nanoscale core-shell micelles on contact with water through a simple dialysis process [15]. Interestingly, there is consistently only one PEG per poly(TMCC-*co*-LA) backbone, giving this polymer a block-like structure. Moreover, the polymeric nanoparticles have demonstrated stability in blood serum proteins in vitro [17]. We hypothesized that these poly(TMCC-*co*-LA)-*g*-PEG nanoparticle micelles would be beneficial in vivo, where the hydrophobic inner core would load a hydrophobic chemotherapeutic drug for delivery, and the PEG corona would reduce protein binding and thereby allow longer circulation and greater tumour accumulation before elimination by the reticuloendothelial system (RES) [9].

Biologically active anti-cancer drugs are often hydrophobic, bulky, and polycyclic, leading to poor aqueous solubility and limited utility [18]. Consequently, such compounds are often formulated with organic co-solvents and surfactants, each with their own systemic toxicities. Docetaxel (DTX) is a small molecule taxane drug that falls into this category: it demonstrates excellent clinical activity against breast cancer but requires a high concentration of polysorbate 80 (PS80 or tween 80) to solubilize relevant concentrations for dosing. Unfortunately, dosing these levels of PS80 causes hypersensitivity reactions, necessitating pre-treatment with corticosteroids and further reducing the mean tolerable dose [19–21].

To take advantage of the potency of DTX without being limited by current formulations, we endeavoured to encapsulate it in the poly(TMCC-*co*-LA)-*g*-PEG nanoparticles, taking advantage of its solubility in the hydrophobic core of our polymeric nanoparticles (Fig. 1). Importantly, this methodology required neither chemical modification nor the use of toxic co-solvents in the final formulation. Success here allowed us to test, for the first time, these polymeric nanoparticles in terms of the in vivo circulation and biodistribution of DTX vs. standard formulations.

To understand the pharmacokinetic behaviour and biodistribution of DTX-loaded nanoparticles (DTX-NP), we compared their performance vs. free DTX in the conventional ethanolic PS80 formulation after dose matched IV injection in tumour-bearing mice. Solid orthotopic tumours were established by transplanting human breast cancer cells into the mammary fat pads of female mice. Ultra performance liquid chromatography-coupled with mass spectrometry (UPLC-MS) detects the unaltered therapeutic compound without labelling, making it possible to distinguish the active compound from inactive fragments, metabolites, or uncoupled tags. This analytical technique is quantitative, sensitive to nM levels, and compatible with small sample volumes [22]. While radiolabeling is commonly used to quantitatively track a drug in tissues and plasma after dosing [23], it relies on a tag as a reporter, and degradation products from the tagged compound can result in misleading data. The UPLC-MS method used here allowed us to directly measure the concentrations of unmetabolized DTX in plasma and tissues after intravenous (IV) injection. Blood samples were drawn via tail vein or cardiac puncture. Using UPLC-MS, we quantified DTX concentrations in the plasma fraction over an 8 h time course and calculated pharmacokinetic (PK) parameters for each formulation.

2. Experimental

2.1. Materials

All cell culture materials were purchased from Gibco-Invitrogen (Burlington, ON, Canada). MDA-MB-231-H2N cells and NSG mice were generous gifts from Dr. Robert Kerbel (Sunnybrook Research Institute, Toronto, ON, Canada), which were then maintained or bred in-house. Dialysis membranes were acquired from Spectrum Laboratories (Rancho Dominguez, CA, USA). Docetaxel was obtained through LC Laboratories (Woburn, MA, United States). Poly(TMCC-*co*-LA) was synthesised as previously described [15,24]. Furan-PEG-NH_2 was prepared from 10 kDa Boc-NH-NH-PEG-NHS obtained from Rapp Polymere (Tuebingen, Germany), and grafted to the polymer backbone as previously described [15,24]. The resulting grafted copolymer is shown in Fig. 1. Heparinized capillary tubes were purchased through Sarstedt (Montreal, QC, Canada). All other materials were purchased from Sigma-Aldrich (Mississauga, ON, Canada) and used as received unless otherwise noted.

2.2. DTX concentration measurement

Chromatographic separations were carried out on an ACQUITY UPLC BEH C18 (2.1 × 50 mm, 1.7 μm) column using ACQUITY UPLC system. The mobile phase was 0.1% formic acid in water (solvent A) and 0.1% formic acid in acetonitrile (solvent B). The column was equilibrated for 1 min in 95% solvent A as the starting point for the gradient, dropping to 5% over 4.5 min, holding for 0.5 min, and moving back to 95% in 0.5 min. A Waters Xevo QTof MS equipped with an atmospheric pressure ionization source was used for MS analysis. For quantification, stock standard solutions of the active DTX compound were added to the final appropriate matrix for comparison: 2:1 acetonitrile:water, v/v for nanoparticle suspensions, or precipitated plasma or pooled tissue homogenates as appropriate. Under these conditions the polymer nanoparticles are dissolved, resulting in a combined measurement of both encapsulated and released DTX present in the original sample. The instrument was sensitive to DTX concentrations as low as 5 ng/mL. All values shown are the average of 5 samples with error bars representing their standard deviation. Group means were compared by one-way ANOVA followed by a corrected unpaired *t*-test; differences are denoted by starred symbols ($p < 0.05$). MassLynx 4.1 was used for peak area analysis and WinNonLin was used to obtain pharmacokinetic parameters in a non-compartmental model.

2.3. Free DTX and DTX-NP formulation

An aqueous suspension of DTX-NP was prepared by self-assembly via a simple dialysis process. First, 15 mg of poly(TMCC-*co*-LA)-*g*-PEG and 6 mg of DTX were dissolved together in 1.425 mL of dimethylformamide (DMF). The solution pH was then adjusted with 75 μL of 500 mM borate buffer, pH 9.0. This mixture was then transferred to a 12–14 kDa molecular weight cut off membrane and dialysed a minimum of four times against distilled water over 24 h at room temperature. This process yielded polymeric nanoparticles loaded with 4.2 wt% DTX with a z-average diameter of 80 nm as measured by dynamic light scattering (Malvern, Zetasizer). Just prior to injection, suspensions of DTX-NP were adjusted for physiological salt content by addition of 10× phosphate buffered saline, pH 7.4 (PBS). Free DTX was prepared by first dissolving DTX in a mixture of ethanol and PS80 before final concentration adjustment with PBS (10% ethanol, 7.5% PS80, 82.5% PBS) directly prior to injection.

2.4. Cell maintenance and preparation

MDA-MB-231-H2N cells were maintained in RPMI 1640 culture medium, supplemented with 10% heat-inactivated foetal bovine serum (FBS), 50 units/mL penicillin and 50 μg/mL streptomycin under a humidified 5% CO_2 environment. To prepare cell suspensions for injection, adherent cells were first rinsed with PBS, and then incubated briefly with trypsin-ethylenediamine tetraacetic acid (trypsin-EDTA,

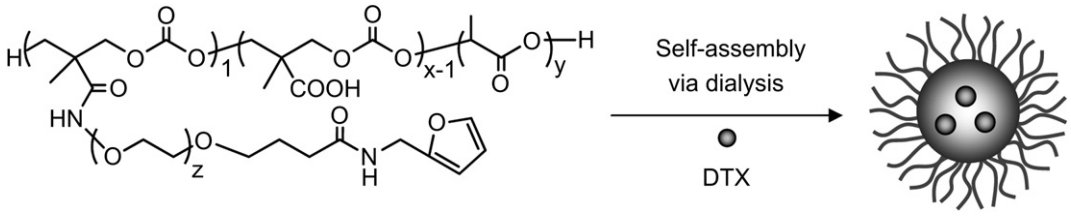

Fig. 1. Poly(TMCC-*co*-LA)-*g*-PEG, shown here with a furan group at the PEG terminus, is an amphiphilic copolymer that self-assembles into polymeric nanoparticle micelles with a core-shell structure on dialysis against water. DTX and the polymer are first co-dissolved in organic solvent before dialysis. During dialysis, DTX partitions into the hydrophobic core, thereby encapsulating it. The polymeric nanoparticles have functional groups available for further modification: carboxylic acid groups on the poly(TMCC-*co*-LA) backbone and furan moieties on the PEG corona.

0.25%/0.038%). Once the cells were suspended, enzymatic digestion was inhibited with FBS, and the cells were pelleted and washed 3 times in PBS before resuspension at the desired concentration. Cells were kept on ice prior to injection.

2.5. Tumour xenograft model

The protocols used in these in vivo studies were approved by the University Health Network Animal Care Committee and performed in accordance with current institutional and national regulations. Animals were housed in a 12 h light and 12 h dark cycle with free access to food and water. NOD scid gamma (NSG) mice were bred in-house, and 7–9 week old female mice were selected for tumour xenotransplantation. To form orthotopic mammary fat pad tumours, mice were inoculated with 10^6 MDA-MB-231-H2N cells suspended in 50 μL of sterile PBS via the following surgical procedures. Prior to surgery, mice were anaesthetized with isoflurane-oxygen. The surgical area was depilated and swabbed with betadine before making an incision in the skin of the lower abdomen to the right of the midline, uncovering the mammary fat pad in the right inguinal region where cells were injected into the fat pad. The incision was then sutured closed and lactated Ringer's solution and buprenorphine were given post-operatively for recovery and pain management. Solid tumours were allowed to form over a period of 3–4 weeks. Cohorts of tumour-bearing animals proceeded onwards for testing once their tumours reached an average diameter of 7 mm as measured through the skin using calipers.

2.6. Pharmacokinetics and biodistribution

DTX-NP and free DTX were compared by giving IV doses of 1.5 mg/kg DTX or DTX equivalent as 200 μL tail vein injections into tumour-bearing mice. Groups of 15 mice were randomly assigned to each formulation. These groups were subdivided into 3 groups of 5 mice with terminal end points at 2, 4, and 8 h. Each of these subgroups was placed on a staggered blood sampling schedule such that each mouse was sampled for blood via the tail vein no more than twice; blood samples were collected using heparinized capillary tubes and immediately centrifuged to collect the plasma fraction. At each terminal time point, animals were sacrificed by CO_2 asphyxiation, and blood was collected via cardiac puncture using heparinized needles and the plasma fraction was immediately isolated by centrifugation. Tissue samples (heart, lung, liver, kidney, spleen, tumour) were also collected by dissection and placed separately in vials. All plasma and tissue samples were snap frozen immediately after collection and kept on dry ice before transfer to −80 °C for long term storage.

2.7. Plasma preparation

To prepare samples for UPLC-MS, plasma samples were thawed and immediately combined with twice their volume in acetonitrile to induce protein precipitation. The supernatant was transferred to an MS vial and stored at 4 °C until analysis. The plasma concentration of DTX was calculated by comparison against blank plasma samples that were spiked with a known concentration of DTX (125–2000 ng/mL as a two-fold dilution series).

2.8. Tissue preparation

Tissue samples were first thawed, accurately weighed, and transferred to vials containing beads for homogenization (zirconia beads for spleen samples, stainless steel beads for all remaining tissue samples). Based on the weight, a multiple of that amount was recorded and added in distilled water (2× for each spleen vial, or 2–4× to a minimum 600 mg total weight in each of the remaining vials) to facilitate homogenization. Samples were then vigorously agitated 3 times in 30 s on/30 s off intervals using a bead beater instrument to mechanically disrupt the tissues. Aliquots of tissue homogenate were transferred into tubes containing double the volume in acetonitrile for protein precipitation. The supernatant was transferred to an MS vial and stored at 4 °C until analysis. The tissue concentration of DTX was calculated by comparison against blank tissue homogenate samples that were spiked with a known concentration of DTX (125–2000 ng/mL as two-fold dilutions) and adjusted for the applied dilution factor.

3. Results

3.1. Pharmacokinetics

Following IV injection, drug compounds distribute through the body and are in turn metabolized and eliminated, and these processes can be modelled with pharmacokinetic parameters using the plasma profile. Both polymeric and conventional formulations exhibited a sharp initial drop in plasma concentration (Fig. 2), with nearly 90% of the detectable DTX dose leaving circulation within 10 min. The steep initial decrease in plasma DTX concentration

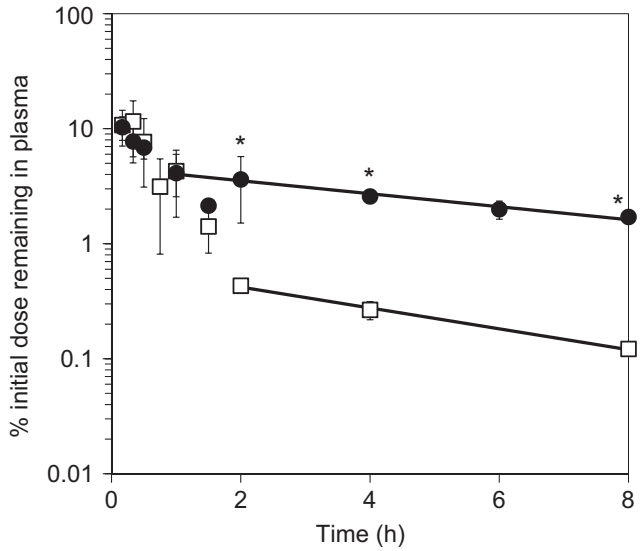

Fig. 2. Pharmacokinetic profiles of free DTX (□) and DTX-NP (●) in tumour-bearing mice. The plasma profiles differ significantly by 2 h post injection. The DTX-NP formulation reached its terminal elimination phase earlier, and coupled with a slower terminal elimination rate, the enhanced plasma retention continued to amplify over time. Points shown are the mean of $n = 5$ animals, with error bars representing their standard deviation. Starred points represent statistically different group means ($p < 0.05$).

observed for both polymeric nanoparticle and standard formulations is characteristic of bolus dosing followed by rapid distribution to surrounding tissues [25]. Metabolic processes likely also contributed because only the intact compound was measured. Remarkably, the plasma profiles diverged significantly at 2 h post injection, with the DTX-NP formulation stabilizing at its terminal elimination phase by 1 h, while the free DTX formulation continued its initial rapid distribution phase until 2 h. By 2 h post injection, the performance of the DTX-NP formulation exceeded that of the free DTX formulation by producing a greater than 8-fold plasma concentration difference (3.62% vs. 0.43% initial dose remaining), widening to a 14-fold difference by 8 h (1.71% vs. 0.12% initial dose remaining).

The improved circulation properties of the polymeric nanoparticle formulation were also reflected in the formulation's pharmacokinetic parameters (Table 1). Even at early times, the modelled initial plasma concentration, C_o, which accounts for the instantaneous dilution due to distribution, was maintained at higher levels for the DTX-NP formulation vs. free DTX, despite the doses being matched at 1.5 mg/kg. For each formulation, the volume of distribution, V_d, was calculated to reflect the theoretical volume over which the DTX is evenly distributed after injection. The calculated V_d for the DTX-NP formulation was half of that for free DTX, further indicating greater retention of active DTX in plasma circulation when delivered by polymeric nanoparticles.

The terminal portions of each plasma profile further distinguished the two groups. Owing to the 1.6-fold longer lambda half life, $t_{,1/2,\lambda}$, for the DTX-NP group, the profiles continued to diverge as more time elapsed. The increasing concentration differences at later times profoundly impacted the pharmacokinetic measures of drug exposure: *AUC* (area under the curve) and *AUMC* (area under the first moment curve). Indeed, the *AUC* for concentration vs. time for the DTX-NP group showed a greater than 2-fold increase over the 8 h observation period, and a greater than 3-fold increase when the duration was extended to infinite time relative to free DTX. Plasma concentrations at later times had an amplified impact on the *AUMC* for concentration × time vs. time and this value

Table 1
Pharmacokinetic parameters calculated for DTX formulations after bolus IV administration of 1.5 mg/kg DTX to tumour-bearing mice.

Pharmacokinetic parameter		Units	Formulation	
			Free DTX	DTX-np
C_o	Initial plasma concentration	ng mL^{-1}	1.47×10^3	1.87×10^3
V_d	Volume of distribution	mL kg^{-1}	4.59×10^3	2.17×10^3
$t_{1/2,\lambda}$	Lambda half-life	h	3.32	5.33
AUC_{all}	Area under the curve (to $t = 8$ h)	h ng mL^{-1}	1.49×10^3	3.52×10^3
AUC_∞	Area under the curve (to $t = \infty$)	h ng mL^{-1}	1.57×10^3	5.31×10^3
$AUMC_\infty$	Area under the first moment curve (to $t = \infty$)	h^2 ng mL^{-1}	2.55×10^3	3.82×10^4
Cl	Clearance	mL h^{-1} kg^{-1}	958	282

increased by an order of magnitude for the DTX-NP formulation vs. the conventional free DTX formulation. The clearance, *Cl*, is a measure of the blood volume that is processed and completely cleared of the injected compound over time. *Cl* decreased by more than 3-fold when DTX was formulated in polymeric nanoparticles vs. conventional PS80. This dramatic decrease suggests that encapsulated DTX is more slowly metabolised and excreted by the body. The fold changes in *AUC*, *AUMC*, V_d, and *Cl* values reported here are all consistent with the ranges published elsewhere for polymeric and liposomal DTX delivery systems [26–31]. In addition to demonstrating similar biodistribution, our polymeric nanoparticles have the advantage of having functional groups available for facile water-based chemistry, allowing further modification [15]. Overall, our pharmacokinetic analysis indicates that with the same initial DTX dose, greater drug exposure was achieved when the drug was formulated in polymeric nanoparticles vs. conventional surfactants, which have the added disadvantage of being cytotoxic and dose-limiting. As a result, the enhanced drug circulation time increased the number of passes through the hyperpermeable tumour vasculature and likely promoted tumour accumulation.

3.2. Biodistribution

To evaluate how encapsulation in our poly(TMCC-*co*-LA)-*g*-PEG nanoparticles affects tissue distribution of DTX, a panel of organs from the same experimental groups were harvested at the sacrificial time points. These samples were later homogenized and assayed for DTX content by UPLC-MS. Nanoparticle formulations often accumulate in the organs rich in RES cells, such as the liver and spleen. Remarkably, there was no significant enhancement of DTX levels in the RES organs resulting from nanoparticle encapsulation (Fig. 3A and B). While accumulation in RES organs was expected, the observation that uptake was not increased in the liver or spleen, relative to free DTX formulations, suggests that the PEG layer on the nanoparticle surface was successful in moderating the RES response [27].

Organs that are active in filtration, such as the lungs and kidneys, are also common sites for nanoparticle accumulation. Filtration through the lungs resulted in high initial entrapment of DTX for both the conventional and nanoparticle formulations, followed by rapid elimination, with no significant differences between group means (Fig. 3C). The lungs often act as a filter for particles as the first capillary bed encountered after tail vein injection [32]. Consequently, the lungs did show the highest DTX concentration of all the organs tested at 2 h post injection, but there were no significant differences between group means, and the concentrations rapidly declined at similar rates. This suggests that a portion of each formulation became transiently entrapped in the lung tissue, possibly due to larger nanoparticles or aggregates, but these particles (of free drug or drug-loaded nanoparticles) subsequently cleared. The kidneys also acted as filters for the injected DTX, which was observed in particular with the DTX-NP formulation, with significantly elevated DTX accumulation in the kidneys throughout the 8 h period of observation (Fig. 3D). Although increased concentrations of DTX in the kidneys were detected for the DTX-NP formulation, the elimination rate constant was higher (1.3-fold increase), resulting in a projected convergence to a level equal to that of the free drug by 24 h.

The next tissue analysed was the heart, where little accumulation was expected. The nanoparticle formulation trended towards a reduced heart accumulation at the early 2 h time point (Fig. 3E); although the difference was not significant, a large variance was observed for the free DTX formulation at the 2 h post injection measurement, and a general upward trend for heart accumulation at this early time.

Significantly greater tumour retention was observed when DTX was encapsulated in nanoparticles starting at 4 h, and maintained at 8 h post injection (Fig. 3F). Indeed, when the tumour accumulation data were fitted with a first order decay, DTX-NP had a greater than five-fold lower elimination rate constant than free DTX, demonstrating significantly greater accumulation of DTX as a result of its delivery in the nanoparticles. This divergence of tissue accumulation was uniquely observed in the tumour and demonstrates the benefit of DTX delivery in nanoparticles.

4. Discussion

We designed the amphiphilic poly(TMCC-*co*-LA)-*g*-PEG to self-assemble into nanoparticle micelles, where the hydrophobic biodegradable core of poly(TMCC-*co*-LA) allows for hydrophobic drug encapsulation and the hydrophilic corona of PEG permits longer circulation time by reducing protein adsorption and cellular recognition. PEG has been shown to be critical design parameter for longer circulation: early particle formulations without PEG demonstrated that particulate drug delivery systems were completely eliminated from circulation within seconds to minutes [33]. The goal of longer circulation is to achieve greater and selective tumour accumulation. In fact, additional passes through the hyperpermeable vasculature associated with solid tumours generally enhances tumour accumulation [34,35]. Enhanced circulation of our DTX-NP was verified using standard PK parameters, demonstrating that greater exposure was achieved with this formulation, even in this model where there was a single injection of a fixed dose. Importantly, enhanced circulation may also increase systemic exposure and general toxicity because drug activity is not limited to cancer cells. As a result, there is a compromise between these opposing factors that requires a balance between high tumour accumulation and low systemic distribution [36]. Importantly, we observed both longer circulation and greater tumour accumulation of these polymeric nanoparticles.

The overall distribution profile of the DTX-NP formulation is encouraging, as the poly(TMCC-*co*-LA)-*g*-PEG nanoparticles established a strong contrast between accumulation in diseased tumour tissues and clearance from healthy tissues, likely due to their engineered material properties. For example, the low critical micelle concentration, measured at 3 μg/mL [15], exceeds the injected concentration by three orders of magnitude, which likely allowed a significant portion of polymeric nanoparticles to circulate intact, instead of rapidly disassembling after dilution in blood. The serum stability of poly(TMCC-*co*-LA)-*g*-PEG nanoparticles has also been confirmed in vitro using biologically relevant media, further suggesting high stability of the nanoparticles and their encapsulated load in circulation [17]. PEG itself has several important

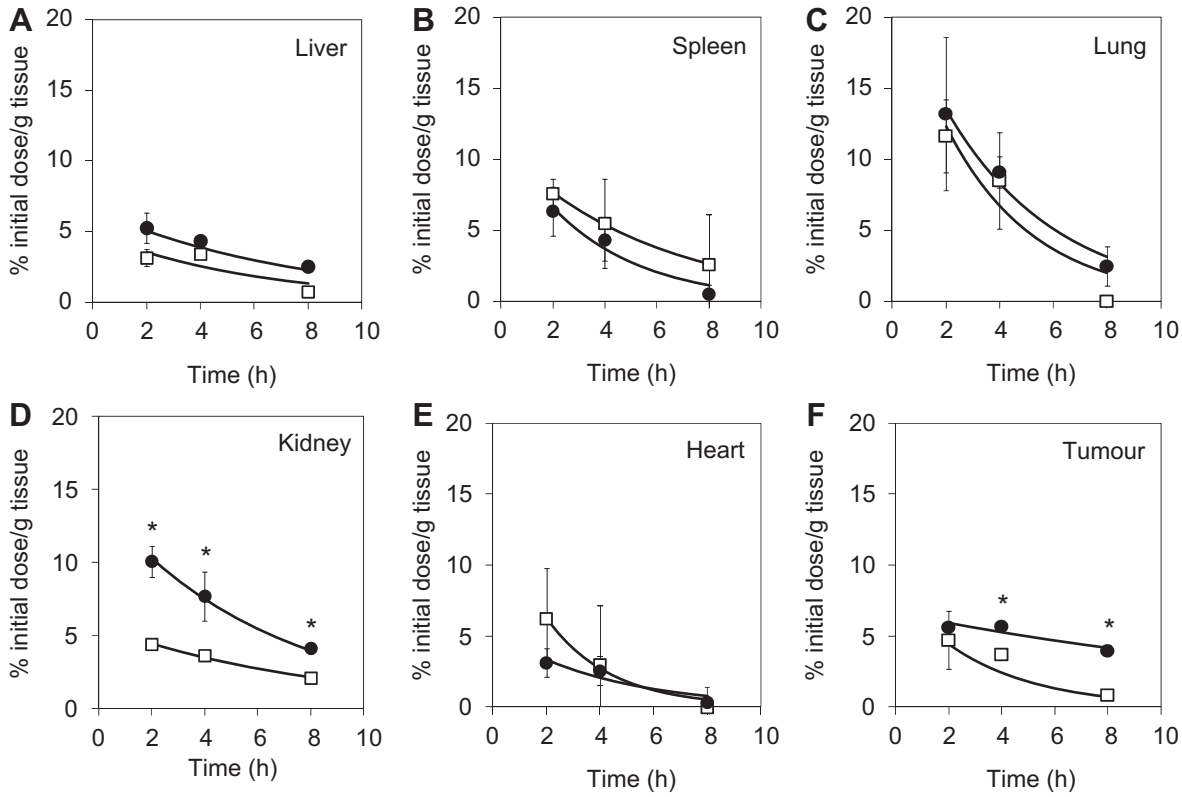

Fig. 3. Biodistribution profiles of free DTX (□) and DTX-NP (●) in (A) liver, (B) spleen, (C) lung, (D) kidney, (E) heart, and (F) tumour tissue. Points shown are the mean of $n = 5$ animals, with error bars representing their standard deviation. Starred points represent statistically different group means ($p < 0.05$).

properties. Firstly, the 10 kDa molar mass exceeds the typical 1–5 kDa range that is commonly used, lowering the PEG density required to reach the more effective brush regime for enhanced circulation [37,38]. Liposomal systems are limited to lower PEG molecular weights because longer PEG chains compromise liposomal stability. Polymeric systems, such as our poly(TMCC-*co*-LA)-*g*-PEG nanoparticles, can stably incorporate higher molar mass PEG by manipulating the molar mass of the hydrophobic region [12]. Secondly, each poly(TMCC-*co*-LA) chain is modified with an average of one PEG chain [15], leading to excellent coverage of the nanoparticle core, which is further reflected by the nearly neutral surface charge of the assembled nanoparticles [16]. Thirdly, the amide bond between PEG and poly(TMCC-*co*-LA) is one of the more serum-stable bonds [39], ensuring lasting nanoparticle coverage after injection. While all particle systems are ultimately cleared, ideally adequate tumour accumulation is reached prior to clearance. This process is normally triggered by degradation or erosion of the polymer comprising the nanoparticle [32]. The poly(TMCC-*co*-LA)-*g*-PEG nanoparticles are subject to eventual erosion because the polymer chains are not cross-linked. The polymer chains are of sufficiently low molar mass (<30 kDa) to be cleared by the kidneys [40] and are themselves biodegradable. These design elements each provide qualities that favour solid tumour drug delivery while minimizing systemic accumulation.

Thorough biodistribution analysis allowed us to quantify the final concentration of DTX in different organs. Notably, DTX did not accumulate in RES organs (liver or spleen) over free DTX controls, suggesting that the inclusion of PEG successfully reduced the expected RES response to foreign particles. The DTX-NP formulation did increase the kidney accumulation over free DTX, pointing to a partial shift to renal clearance, where free DTX is mainly metabolised and excreted by biliary clearance [41,42].

Analysis of the heart demonstrated lower variability of DTX accumulation when administered via polymeric nanoparticles vs. as free DTX. In clinical use, taxanes such as DTX are commonly paired with doxorubicin to treat metastatic breast cancer, but cardiotoxicity is a primary side effect of this drug combination. When used in combination therapy, their administration is staggered, thereby lowering concurrent levels of both drugs to reduce this interaction and reducing cardiotoxicity [43]. Consistently lower initial accumulation in the heart (as was observed with DTX-NP) may allow increased flexibility in the dosing schedule without the risk of introducing severe cardiotoxicity.

The tumour specificity of the DTX-NP formulation is of particular interest. The greater retention of DTX in the tumour when delivered in our polymeric nanoparticles is consistent with the EPR effect observed with other particulate systems. Because this behaviour was uniquely observed in the tumour tissue, there is potential for specific cytotoxic impact on cancer cells while the drug compound is eliminated from the rest of the body. Our system also compared favourably with radiolabeled liposomal DTX formulations: the latter delivered DTX and/or its metabolites to subcutaneous tumours at levels between 2 and 8% initial dose/g, 6 h post injection, depending in the extent of PEGylation [27], whereas our DTX-NP delivered 5% initial dose/g at 6 h post injection based on fitted values from a first order decay for DTX-NP. Similarly, folate targeted PEGylated liposomes achieved 7% initial dose/g of non-degraded DTX 4 h post injection to intradermal tumours measured by LC-MS [28], vs. our 6% initial dose/g for DTX-NP at 4 h.

Indeed, our polymeric nanoparticle formulation delivered an active anti-cancer drug to solid tumours with improved retention over the free drug alone, and this has important implications for anti-tumour efficacy. By extending the drug exposure of diseased

cells, the required cumulative dose will likely decrease, as DTX cytotoxicity depends on both concentration and contact time [44]. Moreover, the dose used in this study (1.5 mg/kg) is consistent with DTX levels administered in metronomic dosing schedules in ovarian cancer models, where several small doses were given at high frequency [45]. This strategy is in contrast with mean tolerated dose approaches, where the highest tolerated dose is given at low frequency to allow healthy tissues to recover between treatments. Metronomic dosing was shown to reduce both systemic toxicity and cumulative dose while improving anti-tumour efficacy, under the premise that the cancer cells have less recovery time between dosing. In combination with more sustained drug levels at each dose, the polymeric nanoparticle formulation offers great potential to demonstrate improved efficacy as a result of greater targeting. Moreover, the nanoparticle DTX delivery system obviates the use of conventional surfactant-based delivery systems which themselves are cytotoxic and cause systemic toxicity.

5. Conclusions

Nanoparticle formulations for anti-cancer drugs are designed to couple specific tumour tissue accumulation with quick elimination from healthy organs. Our DTX-loaded poly(TMCC-*co*-LA)-*g*-PEG nanoparticles achieved this with increased DTX accumulation in the tumour and simultaneous DTX clearance from other organs to which it distributed over an 8 h period of observation. The pharmacokinetic profile of the polymeric nanoparticle formulation vs. free DTX demonstrated improved circulation properties at later times, which likely contributed to the favourable tumour accumulation of DTX when delivered via our engineered formulation. The specific retention of DTX in tumour tissue suggests that this polymeric nanoparticle delivery strategy will be efficacious against solid tumours.

Acknowledgements

We thank: Drs. Robert Kerbel (Sunnybrook Health Science Centre), Armand Keating and Yoko Kosaka (Princess Margaret Hospital) for their help and advice in establishing the mouse tumour model; and Mr. Peter Poon (University of Toronto) for help in growing the tumours and obtaining serum and tissue samples. We are grateful to the Canadian Institutes of Health Research (CIHR to MSS, RSA) the Ontario Centres of Excellence (OCE to MSS), the Ontario Institute for Cancer Research (OICR to RSA), the Natural Sciences and Engineering Research Council (NSERC to KSH), and the Government of Ontario/DuPont Canada Scholarship in Science and Technology (OGSST to KSH) for funding of this research.

References

[1] Cairns R, Papandreou I, Denko N. Overcoming physiologic barriers to cancer treatment by molecularly targeting the tumor microenvironment. Mol Cancer Res 2006;4:61–70.
[2] Dreher MR, Liu WG, Michelich CR, Dewhirst MW, Yuan F, Chilkoti A. Tumor vascular permeability, accumulation, and penetration of macromolecular drug carriers. J Natl Cancer Inst 2006;98:335–44.
[3] Minchinton AI, Tannock IF. Drug penetration in solid tumours. Nat Rev Cancer 2006;6:583–92.
[4] Felici A, Verweij J, Sparreboom A. Dosing strategies for anticancer drugs: the good, the bad and body-surface area. Eur J Cancer 2002;38:1677–84.
[5] Matsumura Y, Maeda H. A new concept for macromolecular therapeutics in cancer-chemotherapy – mechanism of tumoritropic accumulation of proteins and the antitumor agent smancs. Cancer Res 1986;46:6387–92.
[6] Torchilin V. Tumor delivery of macromolecular drugs based on the EPR effect. Adv Drug Deliver Rev 2011;63:131–5.
[7] Mamot C, Drummond DC, Hong K, Kirpotin DB, Park JW. Liposome-based approaches to overcome anticancer drug resistance. Drug Resist Update 2003; 6:271–9.
[8] Majoros IJ, Williams CR, Baker JR. Current dendrimer applications in cancer diagnosis and therapy. Curr Top Med Chem 2008;8:1165–79.
[9] Allen C, Maysinger D, Eisenberg A. Nano-engineering block copolymer aggregates for drug delivery. Colloid Surf B 1999;16:3–27.
[10] Kataoka K, Bae Y. Intelligent polymeric micelles from functional poly(ethylene glycol)-poly(amino acid) block copolymers. Adv Drug Deliver Rev 2009;61: 768–84.
[11] Sahoo SK, Acharya S. PLGA nanoparticles containing various anticancer agents and tumour delivery by EPR effect. Adv Drug Deliver Rev 2011;63:170–83.
[12] Photos PJ, Bacakova L, Discher B, Bates FS, Discher DE. Polymer vesicles in vivo: correlations with PEG molecular weight. J Control Release 2003;90:323–34.
[13] Geng Y, Dalhaimer P, Cai SS, Tsai R, Tewari M, Minko T, et al. Shape effects of filaments versus spherical particles in flow and drug delivery. Nat Nanotechnol 2007;2:249–55.
[14] Sailor MJ, Park JH, von Maltzahn G, Zhang LL, Schwartz MP, Ruoslahti E, et al. Magnetic iron oxide nanoworms for tumor targeting and imaging. Adv Mater 2008;20:1630–5.
[15] Shi M, Wosnick JH, Ho K, Keating A, Shoichet MS. Immuno-polymeric nanoparticles by Diels-Alder chemistry. Angew Chem Int Edit 2007;46:6126–31.
[16] Lu J, Shoichet MS. Self-assembled polymeric nanoparticles of organocatalytic copolymerizated D, L-lactide and 2-methyl 2-carboxytrimethylene carbonate. Macromolecules 2010;43:4943–53.
[17] Lu J, Owen SC, Shoichet MS. Stability of self-assembled polymeric micelles in serum. Macromolecules 2011;44:6002–8.
[18] Torchilin VP. Targeted polymeric micelles for delivery of poorly soluble drugs. Cell Mol Life Sci 2004;61:2549–59.
[19] Aapro M, Bruno R. Early clinical-studies with docetaxel. Eur J Cancer 1995; 31A:S7–10.
[20] Engels FK, Mathot RAA, Verweij J. Alternative drug formulations of docetaxel: a review. Anti-Cancer Drug 2007;18:95–103.
[21] Hennenfent KL, Govindan R. Novel formulations of taxanes: a review. old wine in a new bottle? Ann Oncol 2006;17:735–49.
[22] Xu RNX, Fan LM, Rieser MJ, El-Shourbagy TA. Recent advances in high-throughput quantitative bioanalysis by LC-MS/MS. J Pharmaceut Biomed 2007;44:342–55.
[23] Gupta N, Price PM, Aboagye EO. PET for in vivo pharmacokinetic and pharmacodynamic measurements. Eur J Cancer 2002;38:2094–107.
[24] Shi M, Ho K, Keating A, Shoichet MS. Doxorubicin-conjugated immunonanoparticles for intracellular anticancer drug delivery. Adv Funct Mater 2009;19:1689–96.
[25] Gunaratna C. Drug metabolism and pharmacokinetics in drug discovery: a primer for bioanalytical chemists, part II. Curr Separations 2001;19:87–92.
[26] Esmaeili F, Dinarvand R, Ghahremani MH, Ostad SN, Esmaily H, Atyabi F. Cellular cytotoxicity and in-vivo biodistribution of docetaxel poly(lactide-co-glycolide) nanoparticles. Anti-Cancer Drug 2010;21:43–52.
[27] Khalid MN, Simard P, Hoarau D, Dragomir A, Leroux JC. Long circulating poly(ethylene glycol)-decorated lipid nanocapsules deliver docetaxel to solid tumors. Pharm Res-Dord 2006;23:752–8.
[28] Li X, Tian X, Zhang J, Zhao X, Chen XH, Jiang YH, et al. In vitro and in vivo evaluation of folate receptor-targeting amphiphilic copolymer-modified liposomes loaded with docetaxel. Int J Nanomed 2011;6:1167–84.
[29] Mu CF, Balakrishnan P, Cui FD, Yin YM, Lee YB, Choi HG, et al. The effects of mixed MPEG-PLA/Pluronic (R) copolymer micelles on the bioavailability and multidrug resistance of docetaxel. Biomaterials 2010;31:2371–9.
[30] Upadhyay KK, Mishra AK, Bhatt AN, Castro E, Chuttani K, Dwarakanath BS, et al. In vitro and in vivo evaluation of docetaxel loaded biodegradable polymersomes. Macromol Biosci 2010;10:503–12.
[31] Yuan ZG, Chen DW, Zhang ST, Zheng ZD. Preparation, characterization and evaluation of docetaxel-loaded, folate-conjugated PEG-liposomes. Yakugaku Zasshi 2010;130:1353–9.
[32] Moghimi SM, Hunter AC, Murray JC. Long-circulating and target-specific nanoparticles: theory to practice. Pharmacol Rev 2001;53:283–318.
[33] Gref R, Minamitake Y, Peracchia MT, Trubetskoy V, Torchilin V, Langer R. Biodegradable long-circulating polymeric nanospheres. Science 1994;263:1600–3.
[34] McNeeley KM, Annapragada A, Bellamkonda RV. Decreased circulation time offsets increased efficacy of PEGylated nanocarriers targeting folate receptors of glioma. Nanotechnology 2007;18. Article 385101/385101–385111.
[35] Senthilkumar M, Mishra P, Jain NK. Long circulating PEGylated poly(D, L-lactide-co-glycolide) nanoparticulate delivery of docetaxel to solid tumors. J Drug Target 2008;16:424–35.
[36] Karmali PP, Simberg D. Interactions of nanoparticles with plasma proteins: implication on clearance and toxicity of drug delivery systems. Expert Opin Drug Del 2011;8:343–57.
[37] Nicholas AR, Scott MJ, Kennedy NI, Jones MN. Effect of grafted polyethylene glycol (PEG) on the size, encapsulation efficiency and permeability of vesicles. Bba-Biomembranes 2000;1463:167–78.
[38] Tirosh O, Barenholz Y, Katzhendler J, Priev A. Hydration of polyethylene glycol-grafted liposomes. Biophys J 1998;74:1371–9.
[39] Parr MJ, Ansell SM, Choi LS, Cullis PR. Factors influencing the retention and chemical-stability of poly(ethylene glycol)-lipid conjugates incorporated into large unilamellar vesicles. Bba-Biomembranes 1994;1195:21–30.
[40] Etrych T, Kovar L, Subr V, Braunova A, Pechar M, Chytil P, et al. High-molecular-weight polymers containing biodegradable disulfide bonds: synthesis and in vitro verification of intracellular degradation. J Bioact Compat Pol 2010; 25:5–26.

[41] Bardelmeijer HA, Roelofs ABGH, Hillebrand MJX, Beijnen JH, Schellens JHM, van Tellingen O. Metabolism of docetaxel in mice. Cancer Chemoth Pharm 2005;56:299–306.
[42] Sparreboom A, VanTellingen O, Scherrenburg EJ, Boesen JJB, Huizing MT, Nooijen WJ, et al. Isolation, purification and biological activity of major docetaxel metabolites from human feces. Drug Metab Dispos 1996;24:655–8.
[43] Salvatorelli E, Menna P, Cascegna S, Liberi G, Calafiore AM, Gianni L, et al. Paclitaxel and docetaxel stimulation of doxorubicinol formation in the human heart: implications for cardiotoxicity of doxorubicin-taxane chemotherapies. J Pharmacol Exp Ther 2006;318:424–33.
[44] Hill BT, Whelan RDH, Shellard SA, Mcclean S, Hosking LK. Differential cytotoxic effects of docetaxel in a range of mammalian tumor-cell lines and certain drug-resistant sublines in vitro. Invest New Drug 1994;12:169–82.
[45] Kamat AA, Kim TJ, Landen CN, Lu CH, Han LY, Lin YG, et al. Metronomic chemotherapy enhances the efficacy of antivascular therapy in ovarian cancer. Cancer Res 2007;67:281–8.